

RESEARCH ARTICLE | *Building Neural Circuits: Wiring and Experience*

Binocular deprivation induces both age-dependent and age-independent forms of plasticity in parvalbumin inhibitory neuron visual response properties

Berquin D. Feese, Diego E. Pafundo, Meredith N. Schmehl, and  Sandra J. Kuhlman

Department of Biological Sciences and the Center for the Neural Basis of Cognition, Carnegie Mellon University, Pittsburgh, Pennsylvania

Submitted 25 May 2017; accepted in final form 6 November 2017

Feese BD, Pafundo DE, Schmehl MN, Kuhlman SJ. Binocular deprivation induces both age-dependent and age-independent forms of plasticity in parvalbumin inhibitory neuron visual response properties. *J Neurophysiol* 119: 738–751, 2018. First published November 8, 2017; doi:10.1152/jn.00386.2017.—Activity of cortical inhibitory interneurons is rapidly reduced in response to monocular deprivation during the critical period for ocular dominance plasticity and in response to salient events encountered during learning. In the case of primary sensory cortex, a decrease in mean evoked firing rate of parvalbumin-positive (PV) inhibitory neurons is causally linked to a reorganization of excitatory networks following sensory perturbation. Converging evidence indicates that it is deprivation, and not an imbalance between open- and closed-eye inputs, that triggers rapid plasticity in PV neurons. However, this has not been directly tested in vivo. Using two-photon guided cell-attached recording, we examined the impact of closing both eyes for 24 h on PV neuron response properties in mouse primary visual cortex. We found that binocular deprivation induces a 30% reduction in stimulus-evoked mean firing rate and that this reduction is specific to critical period-aged mice. The number of PV neurons showing detectable tuning to orientation increased after 24 h of deprivation, and this effect was also specific to critical period-aged mice. In contrast to evoked mean firing rate and orientation tuning, measurements of trial-to-trial variability revealed that stimulus-driven decreases in variability are significantly dampened by deprivation during both the critical period and the postcritical period. These data establish that open-eye inputs are not required to drive deprivation-induced weakening of PV neuron evoked activity and that other aspects of in vivo PV neuron activity are malleable throughout life.

NEW & NOTEWORTHY Parvalbumin-positive (PV) neurons in sensory cortex are generally considered to be mediators of experience-dependent plasticity, and their plasticity is restricted to the critical period. However, in regions outside of sensory cortex, accumulating evidence demonstrates that PV neurons are plastic in adults, raising the possibility that aspects of PV response properties may be plastic throughout life. Here we identify a feature of in vivo PV neuron activity that remains plastic past the critical period.

critical period; inhibition; mouse; parvalbumin; vision

INTRODUCTION

The development and plasticity of inhibitory circuits play a central role in determining the timing of critical period plas-

ticity in primary visual cortex (V1) (Hensch 2005; Jiang et al. 2005). In response to monocular deprivation (MD), a decrease in the evoked firing rate of a specific subclass of inhibitory neurons, referred to as parvalbumin-expressing (PV) interneurons, initiates critical period plasticity (Kuhlman et al. 2013). The deprivation-induced reduction in mean firing rate of inhibitory neurons is rapid and precedes changes in excitatory neuron evoked firing rate, thereby invoking a transient state of disinhibition that allows ocular dominance plasticity among excitatory neurons to proceed (Aton et al. 2013; Hengen et al. 2013; Kuhlman et al. 2013). Before the onset of critical period plasticity, PV neuron response properties are immature, in terms of both mean evoked firing rate, which is ~50% lower in the precritical period compared with the critical period, and orientation tuning properties (Kuhlman et al. 2011). Visual experience before the critical period is required for maturation of these response properties to develop, and in adult mice MD does not induce disinhibition. Taken together, these data support a conceptual model in which deprivation-induced disinhibition is permissive, serving to gate the timing of critical period plasticity (Kuhlman et al. 2013). This is in contrast to alternative models proposing that increased inhibition helps to generate an instructive signal during altered sensory experience that suppresses closed-eye inputs (Gandhi et al. 2008; Kuhlman et al. 2010; Yazaki-Sugiyama et al. 2009). A key observable feature of MD-induced plasticity is the differential time course of plasticity between inhibitory and excitatory neurons (Aton et al. 2013; Gandhi et al. 2008; Hengen et al. 2013). This is important, as it sets a window of opportunity for rewiring of excitatory connections such that synaptic weights among excitatory neurons can be updated to reflect new sensory experience. Notably, the rapid cell type-specific reduction in firing rate levels following MD occurs in both binocular and monocular regions of V1 (bV1 and mV1, respectively), indicating that this is a ubiquitous feature of primary sensory visual cortex (Hengen et al. 2013; Kuhlman et al. 2013).

A prediction of this conceptual model is that brief deprivation itself is sufficient to induce rapid plasticity of PV neuron responsiveness and that the reduction in firing rate is specific to inhibitory neurons. We tested this prediction in bV1 as well as mV1 by performing binocular deprivation (BD) and assaying PV responsiveness with two-photon guided cell-attached electrophysiological recording. We found that brief BD induced a 30–40% reduction in mean evoked firing rate specifically in

Address for reprint requests and other correspondence: S. J. Kuhlman, Dept. of Biological Sciences and Center for the Neural Basis of Cognition, Carnegie Mellon Univ., Pittsburgh, PA 15213 (e-mail: skuhlman@cmu.edu).

PV inhibitory neurons and not putative excitatory neurons in bV1 and in mV1. The impact of BD on mean evoked firing was restricted to critical period-aged mice. We also examined the extent to which brief perturbation of vision influences recently developed orientation tuning properties. We found that orientation tuning properties characteristic of mature PV neurons were largely resistant to brief deprivation during the critical period, although we did detect a significant yet subtle effect on the number of PV neurons exhibiting a tuned component. Finally, we considered other analyses beyond mean stimulus-evoked firing rate. Although traditionally mean firing rate averaged across repeated stimulus trials has been extremely useful in understanding cortical development and plasticity, recent studies highlight the need for a more thorough analysis of spike times that takes into account variability across trials. For example, Fano factor analysis of response variability across trials revealed the presence of a cortical state change induced by sensory input. It was observed across a range of brain areas and animals that stimulus onset drives suppression of variable ongoing activity of excitatory neurons. This state change is independent of response magnitude of individual neurons and is therefore likely a property of the local recurrent network (Churchland et al. 2010). The extent to which PV inhibitory neurons also display a stimulus-driven decrease in rate variance in V1 is unknown. Given that PV neurons are highly connected within the local network in terms of the input that they receive, we hypothesized that, similar to excitatory neurons, PV neurons exhibit a stimulus-driven decrease in Fano factor. We found that, indeed, stimulus onset drives suppression of spike rate variability in PV neurons. Furthermore, we found that the magnitude of the stimulus-driven decrease in Fano factor was reduced after BD, and that this reduction occurred in both the critical period and the postcritical period.

Our results provide further evidence supporting a conceptual model in which PV inhibitory neurons gate the timing of critical period plasticity by providing a permissive opportunity for reorganization of excitatory neuron connections, rather than generating an instructing signal. Our examination of spike rate variability revealed a previously unrecognized plasticity in adult PV neurons that may be indicative of a network-level state change inducible throughout life.

MATERIALS AND METHODS

Animal preparation and surgery. All experimental procedures were reviewed and approved by the Institutional Animal Care and Use Committee of Carnegie Mellon University and were compliant with the guidelines established by the National Institutes of Health. Monocular zone experiments were performed in mice expressing cre-recombinase (cre) and red fluorescent protein (tdTomato) in PV neurons derived from the cross between PV-cre knock-in female mice (Jax: 008069, generated by S. Arbor, FMI) and male tdTomato reporter knock-in mice (Jax: 007908, “Ai14,” generated by H. Zeng, Allen Brain Institute). Cell-attached mode recordings were made in left hemisphere visual cortex of 28 urethane-anesthetized mice between ages 25 and 30 days for the critical period experiment and 15 mice between 45 and 60 days for the mature group. Both male and female mice were used. Binocular zone experiments were performed in mice expressing cre and tdTomato in PV neurons derived from the cross between PV-cre knock-in female mice (Jax: 008069, generated by S. Arbor, FMI) and male tdTomato reporter knock-in mice (Jax: 007908, “Ai14,” generated by H. Zeng, Allen Brain Institute) or male

tdTomato reporter congenic knock-in mice (Jax: 007914, “Ai14,” generated by H. Zeng, Allen Brain Institute). Cell-attached mode recordings were made in left hemisphere visual cortex of 16 urethane-anesthetized mice between ages 25 and 31 days. Both male and female mice were used.

Mice that underwent the BD paradigm were anesthetized under isoflurane (3% induction and 1.5–2% maintenance). Silicone oil was applied to both eyes to prevent drying. A single mattress suture (silk 6-0) was made through each eyelid to hold the eye closed. These sutures were made 24 h before the craniotomy surgery and monitored to ensure that closure was maintained. Any mice that showed signs of infection or lid separation were removed from the study.

For surgeries mice were anesthetized with isoflurane (3% induction and 1.5–2% maintenance). Their body temperature was kept constant at ~37.5°C with a heating plate. The eyes of any mice not undergoing BD were protected with silicone oil at the onset of surgery. For mice with eye sutures, their eyes remained sutured shut until ready for recording, at which point the sutures were removed and silicone oil was applied to their eyes. A custom-made stainless steel head bar was affixed to the right side of the skull with ethyl cyanoacrylate glue and dental acrylic, and a silver chloride ground electrode was implanted over the cerebellum. A 1.5- to 2.5-mm craniotomy was made over the left visual cortex. Craniotomies were positioned as described in Kuhlman et al. (2011). A 2.5-mm coverslip was then secured over a portion of the brain with dental acrylic, and cortex buffer (in mM: 125 NaCl, 5 KCl, 10 glucose, 10 HEPES, 2 CaCl₂, 2 MgSO₄) was used to keep the brain moist as well as facilitating imaging.

In vivo cell-attached recording. Mice were sedated with chlorprothixene hydrochloride (5 mg/kg) and anesthetized with urethane (0.5 g/kg). In vivo imaging was performed on a two-photon microscope (Scientifica) imaging system controlled by ScanImage 3 software (Vidrio Technologies; Pologruto et al. 2003). The light source was a Chameleon ultra 2 laser (Coherent) running at 930 nm. A ×40 water-immersion objective from Olympus was used to pass the laser beam. Surface blood vessels, coverslip, and pipette were viewed in visible-light conditions with a green filtered light. Recordings were made 150–350 μm from the pia surface, in layer 2/3.

Pipettes had a resistance of 5–12 MΩ when filled with cortex buffer and 20 μM Alexa Fluor 488 hydrazide (Invitrogen). Labeled neurons were first identified with two-photon imaging. Their *x*, *y*, and *z* coordinates were recorded, and then the pipette was positioned above the neuron's location at low magnification. A Patchstar micromanipulator (Scientifica) was used to back the pipette up an appropriate distance such that moving it in *x* and *z* at a 35° angle would result in it hitting the neuron (roughly 1.73 × the depth of the neuron). The pipette was lowered toward the surface of the brain first under low and then high magnification. The pressure of the pipette was raised to ~200-mbar positive pressure, and a slight increase in resistance marked contact between the pipette tip and the surface of the brain. The pipette was lowered at a 35° angle into the brain, and pressure was reduced to 50 mbar as soon as the dura was penetrated. Once through layer 1, the pressure was reduced to 20–30 mbar until the desired neuron was attained. Two-photon imaging was used to guide the pipette toward the desired neuron, and minor changes in *y* were made as needed. Targeting technique was based on Kuhlman et al. (2011) and Liu et al. (2009). Once the pipette appeared to be touching the neuron, the resistance was lowered and spontaneous spikes could usually be detected. Resistance was decreased to 0, and the pipette was advanced until a 20- to 200-MΩ loose cell-attached seal was obtained. Occasionally, negative pressure was applied up to –50 mbar. Recordings of spontaneous and then evoked spikes were made in current-clamp mode. Signal was acquired with a MultiClamp 700B amplifier in current-clamp mode, a National Instruments digitizer, and WinEDR software (J. Dempster, Strathclyde University). Signal was sampled at 10.02 kHz. Pipette capacitance was compensated.

Visual stimulation. Visual stimulation consisted of full-field square-wave gratings presented at six orientations spaced 30° apart

moving in two directions (12 total stimuli). A temporal frequency of 1 Hz and a spatial frequency of 0.02 cycles per degree (cpd) were used for putative PV neurons, while a temporal frequency of 2 Hz and a spatial frequency of 0.04 cpd were used for putative excitatory neurons. Stimuli were developed with custom software with Psych-Toolbox in MATLAB (MathWorks). Stimuli were presented one at a time in a random order for 3 s at 100% contrast, followed by a 3-s blank gray screen with equal mean luminance. Each stimulus was presented 3–12 times. Stimuli were presented on a 40-cm-wide gamma-calibrated LCD monitor. For monocular zone recordings, the monitor was positioned 25 cm in front of the mouse's right (contralateral to site of recording) eye. The mouse was positioned looking straight forward with a 5–15% rightward tilt to accommodate the brain site for recording being relatively flat. The mouse's nose was approximately aimed toward the left of the screen, with the right eye looking at the center of the screen ± 5 cm right or left. For binocular zone recordings, the monitor was positioned 25 cm in front of the mouse's eyes, with the nose pointed toward the center of the screen. Responses to either contralateral or ipsilateral eye stimulation were interleaved.

Eye shuttering. Eye shuttering was accomplished by placing an occluding device 5 mm in front of the eye. For each eye, an occluding device was constructed of flexible light-blocking material (1.5 cm \times 2 cm) mounted on a flexible linker connected to a vertical post such that either eye could be shuttered or not shuttered in order for each eye to be stimulated.

Data analysis and statistics. Spike waveform analysis was conducted with WinEDR and Clampfit software. For putative PV neurons, the first 50–150 spikes exhibiting good peak (P1) to nadir (P2) amplitudes were averaged and the 10–90% rising and falling slopes as well as P1 and P2 were calculated. For putative excitatory neurons, the first 50–150 spikes (if the neuron fired that many times) were averaged and the 10–90% rising and falling slopes as well as P1 and P2 were calculated. The ratios of P2 to P1 and falling to rising slope were used to normalize for differences in cell-attached resistance across cells.

WinEDR software along with custom-built MATLAB software was used to analyze the firing rate of targeted neurons. The spikes elicited from three runs of the 12 randomly presented stimuli were first sorted. Then the number of spikes elicited over the three runs was averaged for each of the 12 stimuli. The max evoked firing rate was defined as the highest averaged firing rate over the complete number of runs (usually 9 or 12). Tuning curves were obtained by measuring responses to each of the 12 stimuli. The orientation selectivity index (OSI) was calculated with the circular variance (CV) approach, where OSI is defined as $1 - CV$. To generate the estimate of the 95th confidence interval of OSI tuning, an orientation was randomly assigned to each of the gray-screen epochs shown to a given cell (Kuhlman et al. 2011). The mean spontaneous rate for each of the 12 randomly assigned orientations was used to create a tuning curve, and a mock OSI value was calculated. This was repeated 10,000 times to generate a distribution of OSI values, and the 95th two-tailed confidence interval was calculated and displayed as gray shading in Figs. 4 and 5. Given that there was a slight but significant increase in OSI coinciding with a decrease in mean evoked firing rate in BD compared with control animals, it is important to assess whether the observed increase in OSI is an artifact of decreased signal-to-noise ratio (Kuhlman et al. 2011). Although we did not detect a systematic relationship between OSI and firing rate on a neuron-by-neuron basis across the three critical period-age BD conditions ($bV1_{\text{contra}}$, $bV1_{\text{ipsi}}$, $mV1$), one of the three BD experiments ($bV1_{\text{ipsi}}$) did show a significant correlation between OSI and firing rate (Fig. 2A). Therefore we assessed whether the confidence interval for tuning was different across conditions and found that it was not different (Fig. 2). Thus the increase in OSI is not an artifact of lower signal-to-noise ratio in deprived conditions. Bandwidth calculations were based on Ringach et al. (2002), except that a von Mises distribution function was used

to smooth tuning curves and the concentration parameter k was set to 15. After smoothing and baseline subtraction, the orientation angles closest to the peak for which the evoked response equaled $1/\sqrt{2}$ height of the peak response on either side of the curve were estimated. Bandwidth is defined as one-half the difference between these two angles. If the tuning curve did not fall below this criterion, the bandwidth was defined as $\geq 90^\circ$.

Tuning curves were generated by assigning the orientation with the max firing rate over the whole 3 s of stimulus presentation a value of 0 and aligning the rest of the orientations to that. For comparing population tuning curves between control and BD conditions, all firing rates were normalized to the max firing rate of the control condition. For percentage of sample tuned according to OSI, tuned was defined as the OSI value being higher than the OSI calculated based on spontaneous activity of the neuron from the blank gray-screen presentations shown between stimulus presentations (Kuhlman et al. 2011). Even neurons that were tuned according to this definition were still mostly broadly tuned.

Latency to max firing was calculated with 10-ms nonoverlapping bins beginning at stimulus onset. For each 10-ms bin we calculated the firing rate in hertz for that bin over all the given runs. Latency was defined as the middle of the time bin during the first cycle at which the neuron reached its max firing rate. Peristimulus time histograms were made by plotting the firing rates of each 10-ms bin, where 0 is stimulus onset. Raster plots were made by plotting individual spikes of a neuron during each run of the preferred stimulus. Once again, stimulus onset was defined as 0, and 1 s of gray screen response is shown before all 3 s of stimulus response. First and third cycle analysis was performed by averaging the response rate of neurons during the first or third cycle (first or third second since the stimuli were being presented at 1 Hz) of the preferred stimulus presentation, respectively.

Fano factor was computed in MATLAB with code available at <http://churchlandlab.neuroscience.columbia.edu/links.html>. For more in-depth explanation, see Churchland et al. (2010). Spike counts were computed with a 200-ms sliding window moving in 25-ms steps. Variance (across trials) and mean of the spike count were then computed. Fano factor is the spike count variance divided by the spike count mean. The raw Fano factor, which is the slope of the regression relating the variance to the mean, was used. For calculating the difference in Fano factor, a single value was obtained for each neuron by taking the average of the Fano factors during the entire 3 s of gray screen and subtracting from that the average Fano factors during the 3 s of stimulus presentation.

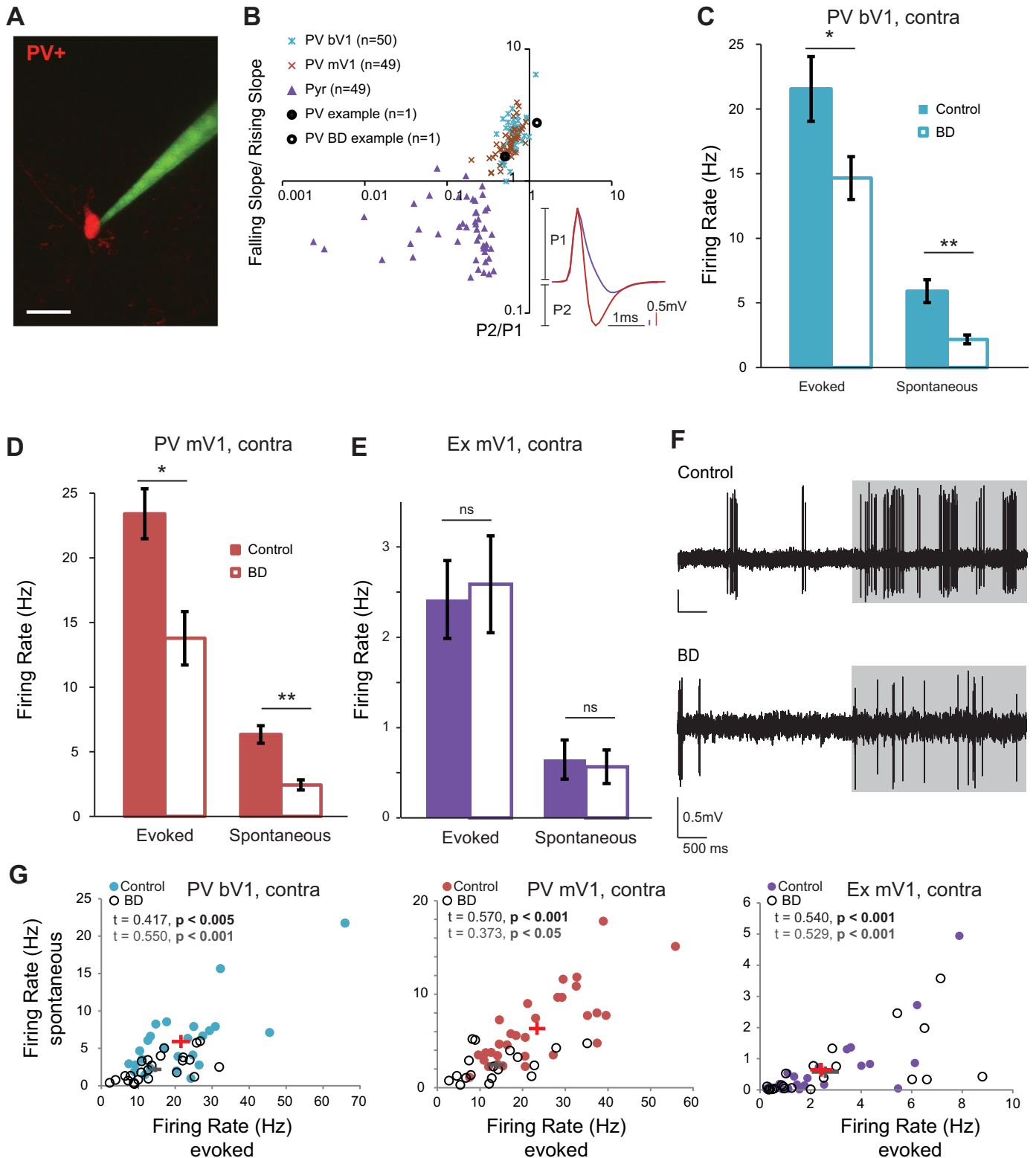
Data are reported as means \pm SE. Data sets were compared with Mann-Whitney U , binomial, or Kolmogorov-Smirnov (K-S) tests as indicated.

RESULTS

Brief binocular deprivation induces reduction of evoked PV neuron firing rate. To understand the effects of BD on PV neurons during the critical period (CP), we performed two-photon guided cell attached recordings from layer 2/3 PV neurons in V1 in mice at age postnatal days (P)25–30 (Fig. 1). Neural activity was recorded in response to drifting gratings, presented at a temporal frequency of 1 Hz at 12 different orientations. The order of stimulus presentation was randomized, and each presentation was interleaved with a gray screen to assess spontaneous activity. The waveform of PV neurons is narrowly shaped (Liu et al. 2009); we used this characteristic to confirm that the correct cell type was targeted (Fig. 1B). We found that 24 h of BD induced a 32% decrease in stimulus-evoked firing rate of PV neurons in the binocular zone ($bV1$), in response to contralateral (contra) eye stimulation, at the

preferred orientation (Fig. 1C; control: 21.55 ± 2.50 Hz, $n = 26$ cells from 9 animals; BD: 14.65 ± 1.65 Hz, $n = 24$ cells from 7 animals; Mann-Whitney U -test $P = 0.025$). Twenty-four hours of BD also caused a significant decrease in the spontaneous firing rate in these same cells (control: 5.91 ± 0.88 Hz; BD: 2.18 ± 0.34 Hz; Mann-Whitney U -test $P < 0.001$). Thus 24 h of visual deprivation is sufficient to

revert both stimulus-evoked and spontaneous firing rates back to immature levels observed during the precritical period (Kuhlman et al. 2011), indicating that continued visual experience is required for critical period-aged neurons to maintain their recently developed firing rate levels. Evoked responses to ipsilateral (ipsi) eye stimulation were also recorded in these same neurons. Similar to $bV1_{contra}$, $bV1_{ipsi}$ evoked responses



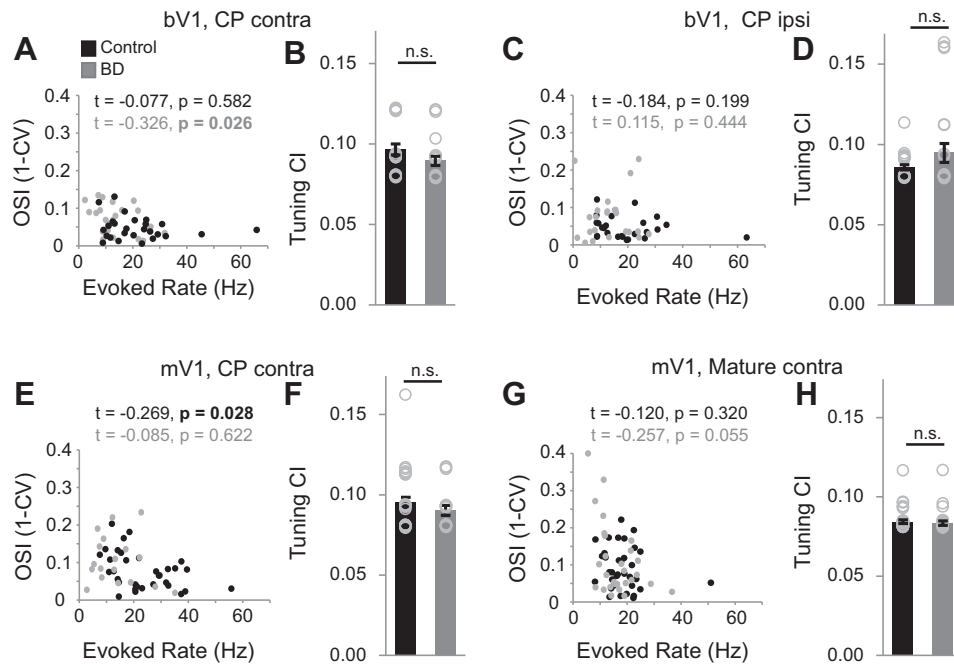


Fig. 2. Evoked spike rates of individual PV neurons in relationship to OSI values. *A, C, E, and G*: Kendall correlation of evoked spike rate and OSI. Significant *P* values are in bold. Brain region, age, and eye stimulation as indicated (bV1 CP_{contra} control: *n* = 26 cells, 9 animals; bV1 CP_{contra} BD: *n* = 24 cells, 7 animals; bV1 CP_{ipsi} control: *n* = 25 cells, 9 animals; bV1 CP_{ipsi} BD: *n* = 23 cells, 7 animals; mV1 CP_{contra} control: *n* = 33 cells, 17 animals; mV1 CP_{contra} BD: *n* = 18 cells, 11 animals; mV1 Mature_{contra} control: *n* = 34 cells, 9 animals; mV1 Mature_{contra} BD: *n* = 28, 6 animals). *B, D, F, and H*: mean 95th confidence intervals (CI) for OSI tuning, averaged across neurons for a given brain region, eye stimulation, and age as indicated. No differences were detected when comparing control vs. BD conditions, indicating that a decrease in signal-to-noise ratio cannot account for the increase in OSI observed after BD in the critical period age group.

were significantly decreased after 24 h of BD (control: 18.88 ± 2.39 Hz, *n* = 25 cells from 9 animals; BD: 13.84 ± 1.56 Hz, *n* = 23 cells from 7 animals; Mann-Whitney *U*-test *P* = 0.0499). To directly confirm that that a rapid decrease in evoked firing rate is a general property of PV neurons in V1 and not restricted to the binocular zone, the experiment was repeated and PV neuron recordings were made in mV1. We found that in mV1 24 h of BD induced a 41% decrease in stimulus-evoked firing rate of PV neurons (Fig. 1*D*; control: 23.40 ± 1.94 Hz, *n* = 33 cells from 17 animals; BD: 13.78 ± 2.06 Hz, *n* = 18 cells from 11 animals; Mann-Whitney *U*-test *P* = 0.002). Again similar to bV1, spontaneous firing rate of the same mV1 neurons was significantly decreased in BD animals compared with control animals (control: 6.03 ± 0.65 Hz; BD: 2.24 ± 0.42 Hz; Mann-Whitney *U*-test *P* < 0.001). Individual neuron responses for all experimental conditions are shown in Fig. 2. As expected from Hengen et al. (2013), in which it was demonstrated that fast-spiking (FS) neuron activity is reduced in mV1 after 24 h of MD, and Kuhlman et al. (2013), in which it was shown that evoked and spontaneous PV neuron activity is reduced in bV1 after 24 h of MD, these results confirm that in both bV1 and mV1 continued

visual experience is required for the recently developed evoked and spontaneous firing rate levels in PV neurons to be maintained.

In addition to PV neurons, a total of 49 putative excitatory neurons were recorded in mV1. We define putative excitatory neurons as neurons that do not express red fluorescence and have asymmetric waveforms compared with PV neurons (Fig. 1*B*). Unlike PV neurons, we did not detect a difference in mean stimulus-evoked firing rate in putative excitatory neurons at their preferred orientation from deprived animals compared with control animals (Fig. 1*E*; control: 2.42 ± 0.43 Hz, *n* = 25 cells from 13 animals; BD: 2.59 ± 0.54 Hz, *n* = 24 cells from 11 animals; Mann-Whitney *U*-test *P* = 0.865). As expected from Hengen et al. (2013), the reduction of activity was specific to PV neurons. However, somewhat unexpectedly, we did not detect an increase in excitatory neuron activity when testing the reopened contralateral eye after deprivation. It is possible that total deprivation caused a reduction in input onto both PV and excitatory neurons but that via network rebalancing due to decreased evoked inhibition (Pouille et al. 2009) the mean evoked firing rate of excitatory neurons did not change. If this were the case, it would be expected that decreased

Fig. 1. Open-eye inputs are not required for rapid plasticity of visually evoked responses in PV neurons. *A*: 2-photon image of recording pipette approaching a parvalbumin-positive inhibitory neuron. Scale bar, 20 μ m. *B*: spike waveforms of inhibitory and excitatory neurons are distinct for all conditions examined. Black circles indicate neurons shown in *F*. *Inset*: average spike waveforms of a parvalbumin-positive inhibitory neuron (red) and a putative excitatory neuron (purple). P1 denotes the amplitude of the spike wave peak, and P2 denotes the nadir. *C* and *D*: evoked and spontaneous firing rates for PV neurons in control (bV1: *n* = 26 cells, 9 animals; mV1: *n* = 33, 17 animals) and BD (bV1: *n* = 24 cells, 7 animals; mV1: *n* = 18 cells, 11 animals) conditions at the preferred orientation in binocular zone (bV1) and monocular zone (mV1) in response to contralateral eye stimulation. **P* < 0.05, ***P* < 0.001 Mann-Whitney *U*-test. *E*: evoked and spontaneous firing rates for putative excitatory neurons in control (filled bars, *n* = 25 cells, 13 animals) and BD (open bars, *n* = 24 cells, 11 animals) conditions at the preferred orientation in the monocular zone. ns, Not significant. *F*: example spike traces; gray shading indicates time of stimulus presentation. *G*: Kendall correlation of evoked and spontaneous firing rates in control and BD (same neurons as in *C–E*). Significant *P* values are in bold (control, black; BD, gray). Data from individual neurons are plotted. Means \pm SE are indicated by red (control) and gray (BD) crosses.

activity would still be detected in the spontaneous activity of excitatory neurons. To address this issue, we examined spontaneous activity of excitatory neurons and did not detect a change in spontaneous firing rate in these same cells (Fig. 1E; control: 0.65 ± 0.22 Hz; BD: 0.57 ± 0.19 Hz; Mann-Whitney U -test $P = 0.384$). In all cases evoked and spontaneous rates were correlated on a neuron-by-neuron basis (Fig. 1G).

PV neuron orientation tuning curves remain broadly tuned after brief deprivation. By the onset of the critical period, PV neuron firing rate increases twofold from that of the precritical period in a vision-dependent manner (Kuhlman et al. 2011). Along with the change in firing rate, there is also a vision-dependent change in orientation tuning curves. PV neurons are more sharply tuned during the precritical period compared with the critical period. In other words, orientation tuning curves become broader with visual experience. We next checked as to whether, similar to firing rate levels, orientation tuning curves are reverted back to the immature state after BD initiated during the critical period. We found that the decrease in evoked firing rate following 24-h BD occurred for all orientations during the critical period; as such, the shape of the tuning curve was not qualitatively altered by deprivation, as can be observed by comparing the mean population tuning curves averaged across all neurons in a given condition for bV1_{contra}, bV1_{ipsi}, and mV1 (Fig. 3). Next, we quantitatively examined tuning curves of individual neurons to determine whether there were subtle changes in tuning properties after brief deprivation. Our analysis revealed that orientation tuning curves for both bV1_{contra} and bV1_{ipsi} conditions remain broadly tuned after brief deprivation. However, a small impact was detected and was significant (Fig. 4). First we considered the global characteristics of the tuning curve by calculating the OSI ($1 - CV$). To define a confidence interval for determining whether an individual OSI value could be considered tuned for orientation, we estimated the 95th confidence interval based on spontaneous firing rate during gray-screen epochs. In this manner, each neuron can be scored as being either tuned or not tuned for orientation. Those neurons with OSI values greater than the confidence interval can be considered tuned. In both control

and deprived conditions the majority of neurons fell below the confidence interval and therefore are most accurately described as being untuned for orientation. We did find, however, that the number of neurons with OSI values above the confidence interval was significantly increased after 24 h of deprivation (Fig. 4, C and E; bV1_{contra} binomial test $P = 0.032$, bV1_{ipsi} binomial test $P = 0.026$).

Next, we considered the local characteristics of the tuning curve by calculating bandwidth. Similar to OSI analysis, in which PV neurons fell into one of two categories (tuned or not tuned), bandwidth can also be categorized as either being untuned ($>90^\circ$) or containing a detectable tuned component ($<90^\circ$). We found that the number of neurons with detectable local tuning significantly increased after brief deprivation (Fig. 4, D and F; bV1_{contra} binomial test $P = 0.003$, bV1_{ipsi} binomial test $P < 0.001$). For those neurons with a bandwidth value of $<90^\circ$, the local tuned component is a continuous variable and can be further analyzed statistically. In the binocular zone we did not find a significant impact of deprivation on the bandwidth value considering only those neurons with a tuned component (Mann-Whitney U -test, bV1_{contra} $P = 0.090$, bV1_{ipsi} $P = 0.227$).

Next, the same analysis was performed on PV neurons in mV1 (Fig. 5). Similar to bV1, in terms of OSI we found that the majority of neurons in the control condition were not globally tuned for orientation and had OSI values less than the confidence interval. Deprivation resulted in a significant increase in the number of neurons tuned for orientation (binomial test $P = 0.041$). Bandwidth analysis revealed that there was also a significant change in the number of neurons containing a detectable tuned component $<90^\circ$ (binomial test $P = 0.024$).

Taken together, bV1 and mV1 PV neurons responded to deprivation in a similar manner; while there were detectable changes in tuning properties, PV neurons remain broadly tuned after deprivation. In addition, we noted a subtle difference between bV1 and mV1. bV1 neurons are slightly more broadly tuned than mV1 neurons in the control condition, before deprivation in terms of OSI (K-S test $P = 0.0132$; Fig. 6A) and

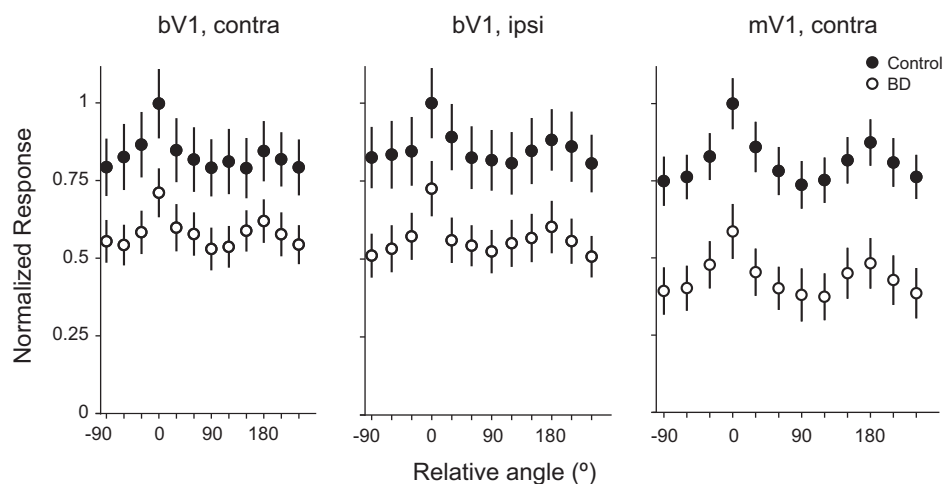


Fig. 3. Deprivation reduces PV neuron evoked responses at all orientations. Orientation tuning curves averaged across neurons for control and BD conditions, brain region (bV1 or mV1), and stimulated eye (contra or ipsi) are indicated. Data are normalized to the mean preferred firing rate of the control population to qualitatively visualize impact of deprivation on orientation tuning (bV1 CP_{contra} control: $n = 26$ cells, 9 animals; bV1 CP_{contra} BD: $n = 24$ cells, 7 animals; bV1 CP_{ipsi} control: $n = 25$ cells, 9 animals; bV1 CP_{ipsi} BD: $n = 23$ cells, 7 animals; mV1 CP_{contra} control: $n = 33$ cells, 17 animals; mV1 CP_{contra} BD: $n = 18$ cells, 11 animals).

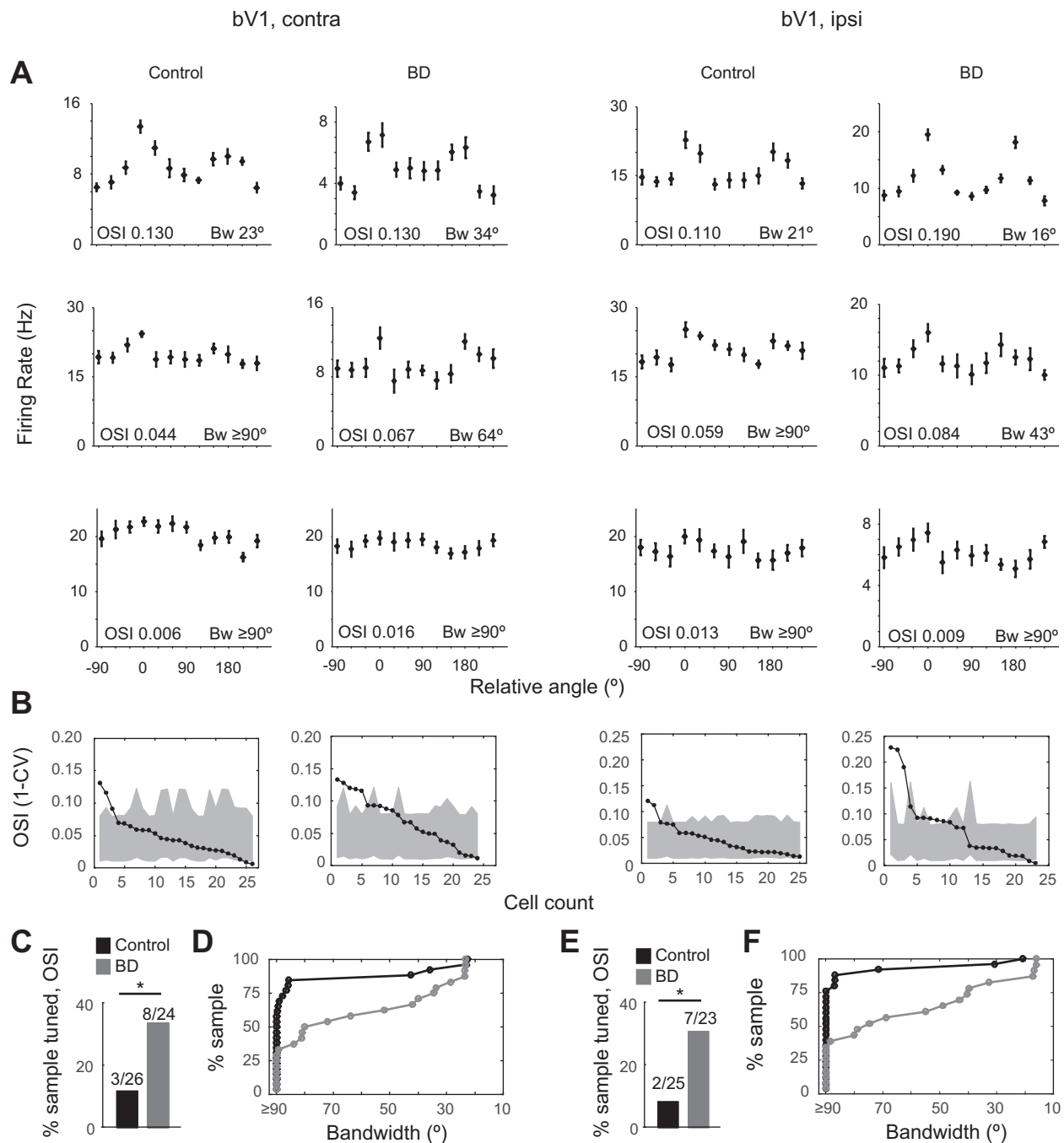


Fig. 4. PV neuron orientation tuning sharpens slightly yet remains broad in bV1 after brief deprivation. *A*: 3 example orientation tuning curves of individual neurons recorded in bV1, covering the range of OSI values observed for control and BD conditions. Eye stimulation is indicated by column label (contra or ipsi). Note that the majority of neurons have OSI values < 0.10 . *B*: summary plot of OSI values of individual neurons, sorted in descending order, along with their individual confidence interval value (gray shading denotes the 95th–5th interval range) (bV1 CP_{contra} control: $n = 26$ cells, 9 animals; bV1 CP_{contra} BD: $n = 24$ cells, 7 animals; bV1 CP_{ipsi} control: $n = 25$ cells, 9 animals; bV1 CP_{ipsi} BD: $n = 23$ cells, 7 animals). Eye stimulation is indicated by column label. Neurons falling above the 95th confidence interval can be considered tuned. *C* and *E*: fraction of neurons with OSI values greater than the 95th confidence interval in control (black) and deprived (gray) conditions. Eye stimulation is indicated by column label. * $P < 0.05$ binomial test. *D* and *F*: cumulative distribution histogram of bandwidth values of individual neurons. Eye stimulation is indicated by column label. Note that the rightward shift following deprivation can be explained by an increase in the number of neurons having a bandwidth value $< 90^\circ$.

bandwidth. Bandwidth analysis revealed that, in contrast to bV1, the majority of mV1 neurons exhibit a tuned component $< 90^\circ$ in the control condition (binomial test $P = 0.043$; Fig. 6*B*). After deprivation, the difference between bV1 and mV1 tuning was reduced, in both OSI (K-S test $P = 0.140$; Fig. 6*C*) and bandwidth (binomial test $P = 0.281$; Fig. 6*D*), although

the rightward shift of the mV1 distribution compared with the bV1 distribution was still present.

Deprivation-induced changes in evoked firing rate and tuning properties are age dependent in mV1. To determine whether V1 PV neurons in postcritical period animals are sensitive to brief deprivation, recordings were made from

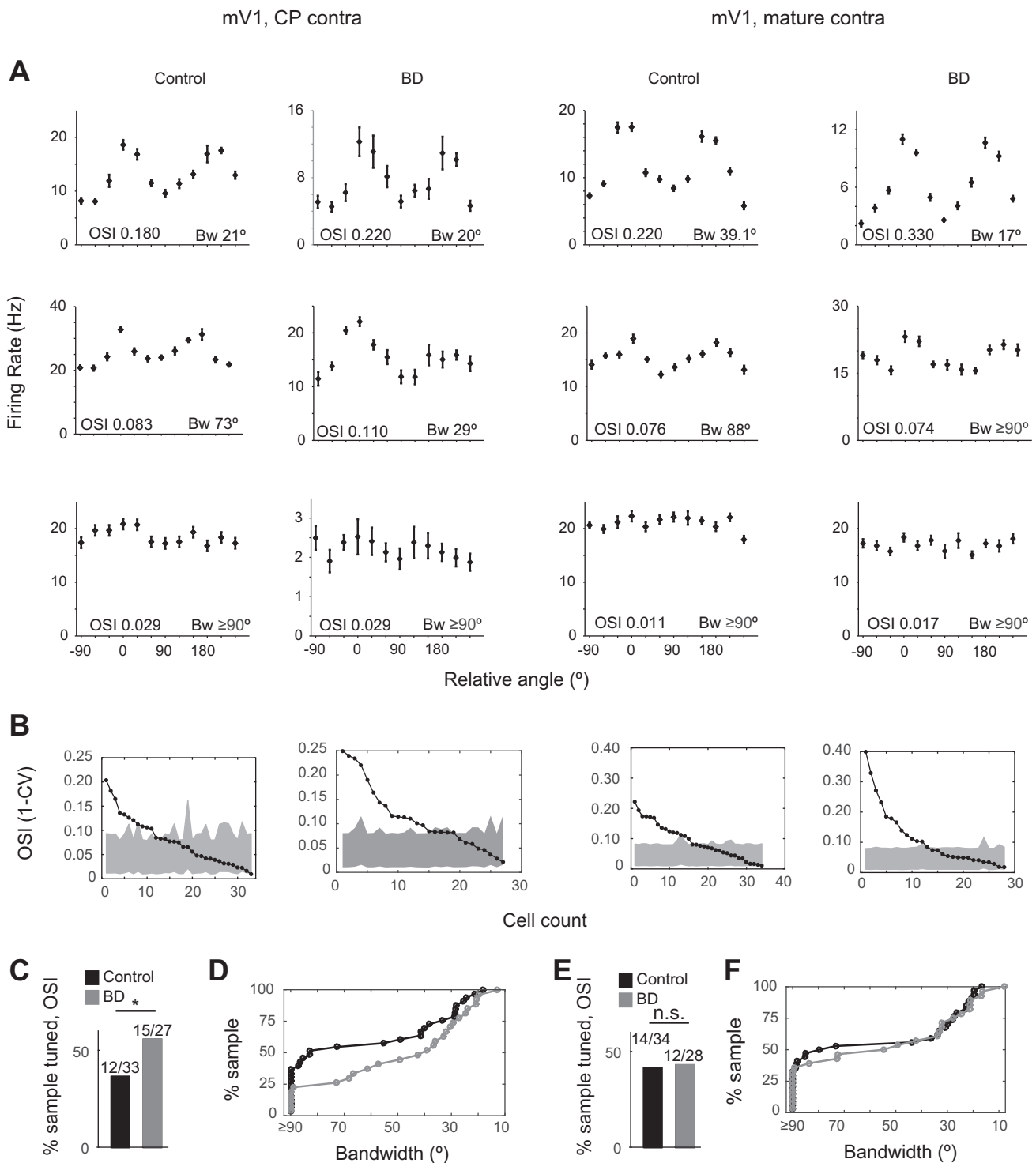


Fig. 5. Deprivation-induced sharpening of PV neuron orientation tuning is age restricted. Data from mV1, plotted as in Fig. 4. Age [critical period (CP) or mature] as indicated by column label (mV1 CP_{contra} control: $n = 33$ cells, 17 animals; mV1 CP_{contra} BD: $n = 27$ cells, 15 animals). * $P < 0.05$ binomial test.

mature mice (P45–65) in mV1. Given that the binocular zone is a more specialized and smaller area compared with the monocular zone and differences between the two areas are known to exist (Lambo and Turrigiano 2013; Nataraj and Turrigiano 2011), our goal was to record from the area most likely to reveal principles of PV neuron development that apply to sensory cortex in general. In contrast to critical period-aged mice, in mature mice we found that mean

stimulus-evoked rates of PV neurons at the preferred orientation did not change after 24 h of deprivation (Fig. 7A; control: 18.37 ± 1.26 Hz, $n = 34$ cells from 9 animals; BD: 16.04 ± 1.26 Hz, $n = 28$ cells from 6 animals; Mann-Whitney U -test $P = 0.120$). Nor did we detect a change in evoked firing rate at the nonpreferred orientations (Fig. 7B). Consistent with this observation, OSI and bandwidth were not altered by brief deprivation in the adult (Fig. 5, E and F).

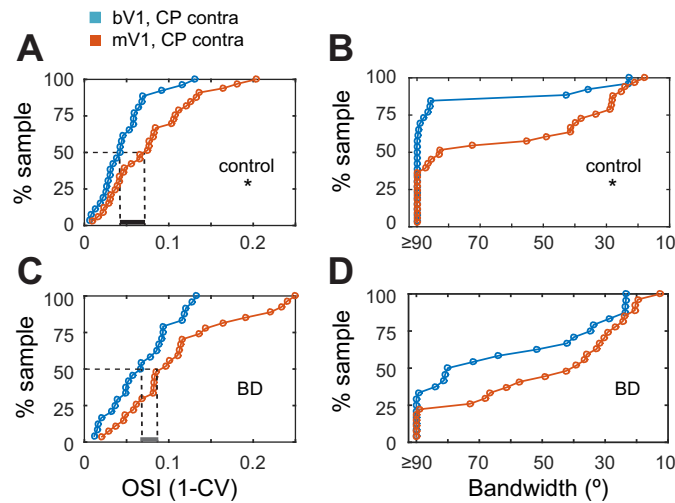


Fig. 6. bV1 neurons are more broadly tuned for orientation than mV1 neurons. Comparison of OSI (K-S test) and bandwidth (binomial test) values between bV1 and mV1 in critical period-aged mice in control and BD conditions. Note that the median OSI values are more similar in the BD condition (dashed lines) compared with control and that the proportion of neurons having a bandwidth $\geq 90^\circ$ is also more similar in the BD condition compared with control (bV1 CP_{contra} control: $n = 26$ cells, 9 animals; bV1 CP_{contra} BD: $n = 24$ cells, 7 animals; mV1 CP_{contra} control: $n = 33$ cells, 17 animals; mV1 CP_{contra} BD: $n = 27$ cells, 15 animals). * $P < 0.05$.

In mature animals, V1 PV neurons are characterized as being the first cell type to respond and their response is strongest during the first stimulus cycle (Ma et al. 2010). Next, we evaluated the extent to which these properties are developed at the time of the critical period (Fig. 8). Latency to reach maximum firing rate was similar between critical period and mature age groups (CP: 389.55 ± 48.9 ms; mature: 315 ± 41.6 ms; Mann-Whitney U -test $P = 0.415$). However, the ratio of first cycle response to third cycle response was not fully developed in critical period-aged mice (CP: 1.45 ± 0.05 ; mature: 1.76 ± 0.12 ; Mann-Whitney U -test $P = 0.014$). Despite this incomplete development at the time of the critical period, deprivation induced a decrease in mean evoked firing rate in both the first and last stimulus cycles (Fig. 8).

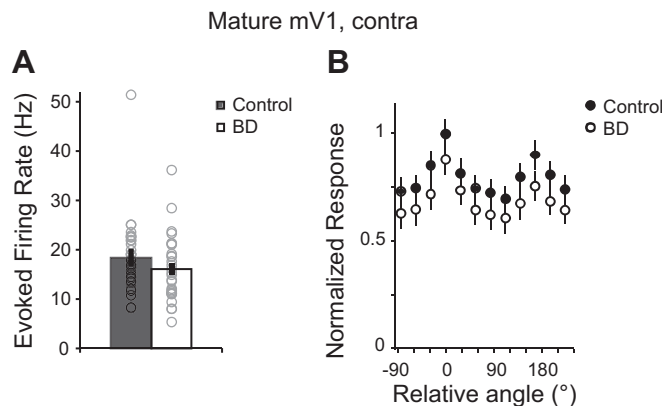


Fig. 7. Evoked firing rates of PV neurons in mature mV1 are not altered by brief deprivation. **A:** evoked firing rates for control and BD conditions of PV neurons at their preferred orientation (mV1 Mature_{contra} control: $n = 34$ cells, 9 animals; mV1 Mature_{contra} BD: $n = 28$, 6 animals). **B:** orientation tuning curves averaged across neurons for the control and BD conditions. Data are normalized to the mean preferred firing rate.

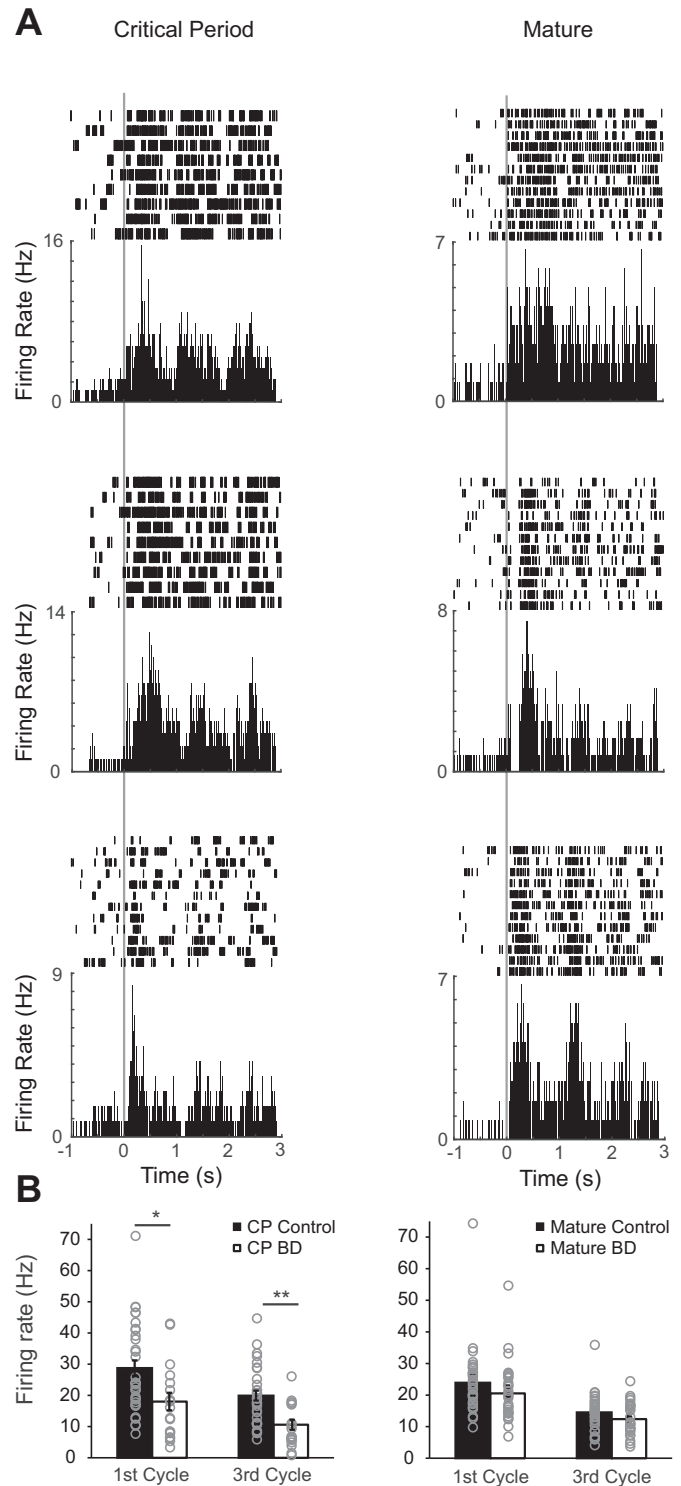


Fig. 8. Deprivation-induced suppression of PV responsiveness is age restricted in mV1. **A:** 3 example raster and peristimulus time histogram plots of individual neurons recorded in mV1. Data are aligned to stimulus onset ($time 0$) as indicated by vertical gray line. Age (critical period or mature) is indicated by column label. **B:** 1st and 3rd cycle evoked firing rates for control and BD conditions of PV neurons at their preferred orientation (mV1 CP_{contra} control: $n = 33$ cells, 17 animals; mV1 CP_{contra} BD: $n = 18$ cells, 11 animals; mV1 Mature_{contra} control: $n = 34$ cells, 9 animals; mV1 Mature_{contra} BD: $n = 28$, 6 animals). * $P < 0.05$, ** $P < 0.001$ Mann-Whitney U -test, Bonferroni corrected for 4 comparisons.

PV neurons exhibit stimulus-induced reduction in variability of spike times. It is becoming increasingly clear that, in addition to altering the trial-averaged firing rate of individual neurons, stimulus onset alters ongoing fluctuations in spontaneous activity of excitatory neurons such that the variability of spike times is dramatically reduced, at timescales of 100–200 ms (Churchland et al. 2010; Poulet and Petersen 2008; Sussillo and Abbott 2009). Notably, the reduction occurs even in response to stimuli that do not elicit a strong mean evoked response, such as occurs in recordings of orientation-tuned neurons presented with a nonpreferred orientation (Churchland et al. 2010). At the population level, it is observed that during sensory stimulation spike time patterns occupy a subspace of possible patterns such that spike patterns during stimulation appear to be constrained by the observed spontaneous activity of the same network (Luczak et al. 2009; Shadlen and Newsome 1998). Together, this is evidence that the population spike patterns that occur during sensory stimulation are drawn from a parameter space of possible patterns observed during spontaneous fluctuations. Sensory responses represent a more narrowly restricted set of patterns and, as such, display lower trial-to-trial variability compared with spontaneous activity. Next, we estimated across-trial variability of PV spike times to assess the extent to which stimulus onset reorganizes the variability of PV neuron spike times. Given that PV neurons are highly connected within the local network, first we hypothesized that, similar to excitatory neurons, PV neurons exhibit a stimulus-driven decrease in variability of spike times.

We assessed across-trial variability by calculating the Fano factor of individual neuron spike times before the stimulus (gray screen presentation, pre) and after stimulus onset (post). Fano factor was computed as the spike time variance divided by the mean firing rate. Assuming spike times follow a Poisson process, which would yield a Fano factor of 1, Fano factor values > 1 can be interpreted as being an indication of cross-trial firing rate variability (Churchland et al. 2006, 2010; Mitchell et al. 2007; Nawrot et al. 2008). In both age groups, the mean Fano factor across animals was reduced at stimulus onset and approached a value of 1 (Fig. 9, A–D; CP: pre 2.75 ± 0.13 , post 1.72 ± 0.10 , Mann-Whitney U -test $P < 0.001$; mature: pre 2.07 ± 0.10 , post 1.27 ± 0.08 , Mann-Whitney U -test $P < 0.001$). The magnitude of reduction, defined as the difference between mean prestimulus and mean post-stimulus Fano factor values averaged over 3 s, was similar for the critical period-aged and mature mice, $31 \pm 4.0\%$ and $37 \pm 3.0\%$, respectively. Thus, similar to excitatory neurons, stimulus onset reduces across-trial variability of PV spike times.

Stimulus-induced reduction in Fano factor occurs in deprived animals. Mechanistically it is unclear what gives rise to the stimulus-induced decline in variability. Decreased variability may be a property of large recurrent networks (Sussillo and Abbott 2009); on the other hand, stimulus-evoked shunting inhibition is well positioned to mediate the decline (Monier et al. 2003). If stimulus-evoked inhibition is a contributing factor, then manipulations that decrease stimulus-evoked inhibition should prevent stimulus onset from driving Fano factor down to a value approaching 1. In other words, decreased inhibition should reduce the magnitude of the stimulus-induced decline in variability such that Fano factor is not reduced to 1. It was previously noted that experimentally it is difficult to test this

prediction (Churchland et al. 2010). Given that BD in critical period-aged mice creates a network state in which PV inhibitory neuron firing rate is decreased but excitatory neuron firing rate is maintained, the prediction can be directly tested in deprived mice. We found that the ability of stimulus onset to drive Fano factor to a value approaching 1 was not disrupted after 24 h of BD in PV neurons (Fig. 9E; CP BD: pre 1.75 ± 0.12 , post 1.36 ± 0.08 , Mann-Whitney U -test $P = 0.026$). These results indicate that stimulus-evoked inhibition from PV neurons is not a major contributing factor to the stimulus-induced decrease in spike time variability. Consistent with this interpretation, the stimulus-induced decrease in Fano factor in adults subjected to 24 h of BD, which do not have altered PV neuron responsiveness, was similar to that of critical period-aged mice after 24 h of BD (Fig. 9F; mature BD: pre 1.52 ± 0.08 , post 1.24 ± 0.08 , Mann-Whitney U -test $P = 0.004$). However, we cannot rule out the possibility that rebalancing of synaptic weights masked an effect on Fano factor in the BD condition. To confirm that Fano factor is reduced specifically at stimulus onset (see also time course in Fig. 9, A and B), we repeated the above analysis for a restricted window of 200 ms before and 200 ms after stimulus onset (CP control: pre 2.67 ± 0.27 , post 1.67 ± 0.16 , Mann-Whitney U -test $P = 0.004$; CP BD: pre 2.18 ± 0.31 , post 1.32 ± 0.16 , Mann-Whitney U -test $P = 0.023$; mature control: pre 1.88 ± 0.14 , post 1.37 ± 0.15 , Mann-Whitney U -test $P = 0.006$; mature BD: pre 1.82 ± 0.25 , post 1.20 ± 0.11 , Mann-Whitney U -test $P = 0.037$).

Unexpectedly, in both age groups after BD there was a decline in spike time variability in the nonstimulated epoch preceding stimulus onset (Fig. 9, G and H, insets; Fano factor values, CP: control pre 2.75 ± 0.13 , BD pre 1.75 ± 0.12 , Mann-Whitney U -test $P < 0.001$; mature: control pre 2.07 ± 0.10 , BD pre 1.51 ± 0.08 , Mann-Whitney U -test $P < 0.001$). Consistent with this observation, the median magnitude of the stimulus-driven decrease in Fano factor (magnitude of reduction, defined above), was significantly reduced after deprivation by 75% and 38% in critical period-aged (K-S test $P < 0.001$) and adult (K-S test $P < 0.001$) mice, respectively (Fig. 9, G and H). These data indicate that brief deprivation alters the spontaneous spike time patterns of PV neurons and that this deprivation-induced change is not restricted to the critical period.

DISCUSSION

PV inhibitory neurons are generally thought to be mediators of experience-dependent plasticity. Despite their central role in postnatal development of sensory processing, systematic studies on the development and sensitivity of their response properties to brief deprivation are lacking. Here we focused on three characteristics of PV neuron development and plasticity. First, we confirmed that the ability of PV neurons to rapidly modify their average firing rate in response to deprivation is a general property of V1 not restricted to the specialized area of the binocular zone and does not require the presence of open-eye inputs. Second, in contrast to evoked firing rate, we found that PV neuron orientation tuning is largely unaltered by brief deprivation during the critical period. Finally, our examination of spike rate variability revealed a previously unrecognized plasticity in adult PV neurons that may be indicative of a network-level state change inducible throughout life.

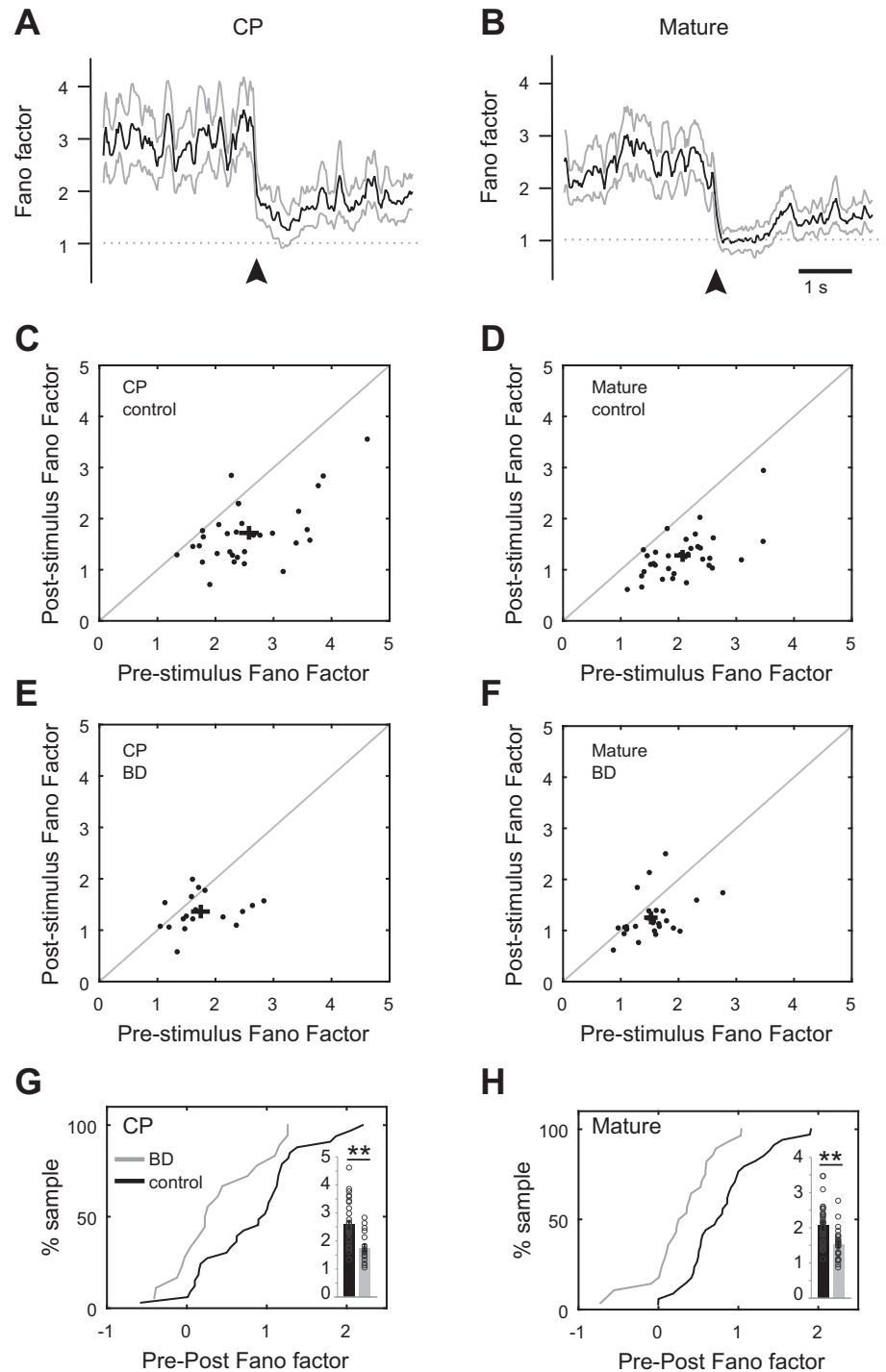


Fig. 9. PV neuron spike time variability during nonstimulus epochs is reduced by deprivation: Fano factor analysis of neural responses to the preferred orientation and the gray screen immediately preceding stimulation (mV1 CP_{contra} control: $n = 33$ cells, 17 animals; mV1 CP_{contra} BD: $n = 18$ cells, 11 animals; mV1 Mature_{contra} control: $n = 34$ cells, 9 animals; mV1 Mature_{contra} BD: $n = 28$, 6 animals). *A* and *B*: sliding average of Fano factor (bold) across the population (binned by 200 ms) before and after stimulus onset (arrowhead). Animal age group is indicated. *C–F*: scatterplots of Fano factor values of individual neurons (binned by 200 ms), averaged across the 3 s of gray screen preceding stimulus (prestimulus) and 3 s of visual stimulation (poststimulus). Animal age group and treatment condition are as indicated. Mean and SE are indicated by black crosses; note the leftward shift of mean prestimulus values in control vs. BD in both age groups. *G* and *H*: cumulative distribution plots of pre – post Fano factor differences for individual neurons. Animal age group and treatment condition are indicated. In both age groups there was a leftward shift after BD. *Insets*: spike time variability in the nonstimulated 3-s long epoch preceding stimulus onset was reduced in both critical period-aged and mature conditions. ****** $P < 0.001$ Mann-Whitney *U*-test.

Deprivation-induced rapid plasticity of PV neurons does not require open-eye inputs. During critical periods of development, cortical connectivity among excitatory neurons is highly malleable. This increased plasticity allows new experiences to shape the neural circuitry used to encode behaviorally relevant information available in the animal's environment such that the neural circuitry is matched to local conditions. Classic MD studies establish that the timing of critical period plasticity is set by the protracted development of cortical PV inhibitory interneurons (Hensch 2005). Two alternative mechanistic explanations as to how inhibition initiates critical period have

been proposed. The first proposed that in response to MD the imbalance of visual input between the two eyes is detected and in response to this imbalance PV neurons shift their ocular dominance away from the open eye such that inhibition becomes relatively stronger in the closed-eye pathway and promotes long-term depression (LTD) and/or suppression of closed-eye inputs. The discovery that PV neurons, which are equally driven by both eyes in control conditions, shift their responsiveness toward the closed eye with 48 h of MD is strong evidence in favor of this conceptual model (Yazaki-Sugiyama et al. 2009). Computational models constrained by

experimental results provide further support of this proposal (Aton et al. 2013; Kuhlman et al. 2010). Alternatively, rather than an imbalance of input between the two eyes being the initiating factor, it has been proposed that deprivation itself is sufficient to cause an overall reduction in PV neuron responsiveness. This proposal is based on the observation that brief MD causes a transient suppression of PV neuron activity in both the closed-eye and open-eye pathways. Consistent with this observation, putative PV neurons identified by their narrow spike waveform recorded in the monocular zone were shown to rapidly suppress their activity within 24 h of contralateral MD in freely moving animals in the monocular zone (Hengen et al. 2013). The transient reduction of PV-mediated inhibition in binocular zone is both required and sufficient for ocular dominance plasticity among excitatory neurons to proceed (Kuhlman et al. 2013). Thus it appears that disinhibiting weak, open-eye inputs during MD creates a temporary permissive environment in which synaptic plasticity can update cortical processing to reflect new sensory conditions (van Versendaal and Levelt 2016). A prediction of the later proposal is that deprivation itself is sufficient to suppress bV1 PV neuron responsiveness, whereas PV neurons would not be expected to alter their response properties after BD if it is an imbalance of input between the two eyes that drives rapid plasticity of PV neuron activity.

Here we tested this prediction by recording PV neurons after BD and found that deprivation is sufficient to drive a decrease in PV neuron responsiveness. From this we conclude that an imbalance of ocular input is not required for PV neurons to alter their responsiveness; these results support the second proposed model. The distinction between these two models is important; an implication of the first model is that there is a biological circuit capable of computationally detecting closed vs. open input pathways. The second model does not require such a pathway-specific detector circuit; rather, in response to deprivation, the network transiently enters a disinhibited state. In this state, despite lower sensory drive the threshold for induction of LTD is maintained. Without disinhibition, it is expected that the threshold for LTD would be increased, because of BCM (Bienenstock, Cooper, and Munro) metaplasticity (Cooper and Bear 2012), and closed-eye inputs would not undergo LTD. Consistent with this model, blockade of disinhibition via infusion of a GABA_A receptor use-dependent agonist during MD blocks ocular dominance plasticity (Kuhlman et al. 2013).

Our study focused on PV neurons, identified by their molecular expression of parvalbumin and functional narrow spike waveform. Using this targeted approach in both bV1 and mV1, we were able to directly address an open question in the literature. Previously it was observed that bV1 inhibitory neurons studied as a general class, identified by the molecular expression of the GABA synthesizing enzyme GAD67, exhibit a delayed shift in ocular dominance after MD (Gandhi et al. 2008). Computationally it was shown in this same study that a transient mismatch or imbalance between inhibition and excitation can promote LTD of closed-eye inputs by suppressing closed-eye inputs. In this view, plasticity of inhibition would be instructive rather than permissive, as are the proposed models discussed above (Aton et al. 2013; Kuhlman et al. 2010; Yazaki-Sugiyama et al. 2009). On the other hand, reports in which putative inhibitory neurons are identified by their

functional narrow spike waveform demonstrate that FS neurons rapidly respond to deprivation in mV1 without delay (Hengen et al. 2013). Our study confirms that FS PV neurons rapidly respond to deprivation in both bV1 and mV1; however, the question of how the other inhibitory GABAergic neuron subtypes, such as VIP- and somatostatin-expressing neurons, shift their eye dominance during deprivation-induced plasticity remains open. Furthermore, the extent to which permissive disinhibition applies to animals with cortical columns and less contralateral bias in excitatory neuron drive, such as the cat, remains unclear. In the case of cats, the data support an instructive model in initial column development and MD (Aton et al. 2013; Hensch and Stryker 2004). In this regard, it is worth noting that the extent to which disinhibition plays a role in MD of the ipsilateral eye in the binocular zone of mice is unknown.

Based on Hengen et al. (2013), we hypothesized that the rapid decrease in PV responsiveness observed in Kuhlman et al. (2013) did not require open-eye inputs. Indeed, as expected, this is what we found. However, although the effect was specific to PV neurons we did not see an increase in excitatory neuron activity. From recent literature, there are three likely possible explanations as to why we did not see an increase in excitatory neuron activity as predicted by Hengen et al. (2013). First, it should be noted that single-eye deprivation and complete deprivation may differentially impact excitatory neurons, even in mV1. Although the monocular zone only receives input from the contralateral eye, in terms of patterns of activity across the visual system, which is reciprocally connected across levels, including the thalamus, V1, and V2 (D'Souza and Burkhalter 2017), it is possible that BD and MD result in distinct patterns of activity across the visual system. Total visual deprivation could decrease input onto both PV and excitatory neurons, and such a decrease in evoked inhibition could mask a decrease in excitatory neurons, for example, by a dynamic gain mechanism (Pouille et al. 2009). While our results on spontaneous activity of excitatory neurons argue against this scenario, more direct *in vitro* studies examining the strength of synaptic input onto PV neurons are needed to establish that, similar to MD (Kuhlman et al. 2013; Stephany et al. 2016; Sun et al. 2016), BD decreases the strength of synaptic input from layer 4 excitatory neurons onto layer 2/3 PV neurons via a signaling mechanism such as the tyrosine kinase neuregulin/ErbB4 pathway (Gu et al. 2016; Sun et al. 2016). Second, BD may be a more potent perturbation of cortical activity compared with MD and lead to a more rapid homeostatic recovery of excitatory neurons to their original firing rate set point (Hengen et al. 2016) such that rather than requiring 2–3 days to recover, excitatory neurons start to recover within 24 h. Finally, unlike Hengen et al. (2013), these studies were performed in anesthetized animals.

In addition to mean evoked firing rate, we found that deprivation had a significant effect on PV neuron orientation tuning, specifically during the critical period. The number of neurons showing detectable tuning increased after brief deprivation. However, this effect was subtle, and perhaps more salient is our finding that the majority of PV neurons remain broadly tuned after deprivation. Thus, in terms of functional impact on sensory processing, the deprivation-induced change in PV tuning is likely minimal; however, mechanistically it

appears that continued visual experience is required to maintain broad tuning during the critical period but not after closure of the critical period. We also found that bV1 PV neurons are detectably more broadly tuned than mV1 PV neurons. The circuit basis for this is unknown. Given that callosal inputs from the contralateral hemisphere preferentially arborize in bV1 compared with mV1 (Wang and Burkhalter 2007), it is possible that callosal input serves to broaden PV neurons in the binocular zone. Interestingly, the difference between bV1 and mV1 was reduced after deprivation; thus the mechanism responsible for generating broader tuning in bV1 appears to be sensitive to deprivation.

Deprivation induces decrease in spike time variability during spontaneous but not visually evoked epochs throughout life. Experimental evidence demonstrates that recent visual experience is reflected in spontaneous cortical activity patterns (Han et al. 2008). Considering Hebbian rules of plasticity, it has been proposed that the spontaneous state's statistics observed in the absence of visual drive may reflect past input statistics as experienced during vision, such that the upper limit of the number of spontaneous spike time patterns that are entered is set by how many patterns were recently experienced during vision. The more spike time patterns present, the higher the variability (Doiron et al. 2016; Litwin-Kumar et al. 2016). Thus an implication of our findings is that 24 h of visual deprivation is sufficient to degrade the number of spike time patterns that spontaneously occur in PV neurons. This is consistent with the view that spontaneous activity is structured in space and time and reflects the underlying network connectivity among neurons (Ringach 2009). Independent of this implication, we were able to demonstrate clearly that a reduction in sensory-evoked inhibition did not impact the ability of stimulus onset to reduce the Fano factor to values approaching 1 in PV neurons. It will be of interest in future studies to determine whether this is also the case for excitatory neurons.

Notably, the deprivation-induced decrease in spike time variability that we observed in the spontaneous state occurred in both critical period-aged and adult mice. Given that PV neurons are well positioned to pool the activity of many neighboring excitatory neurons (Bock et al. 2011), it is possible that our measure of PV neuron spike time variability in the spontaneous state is a readout of the spike time patterns generated by the excitatory network. In this context, our results raise the possibility that the spike time patterns generated by excitatory neurons in the spontaneous state are equally sensitive to deprivation in the critical period and the adult. Alternatively, the changes could be specific and intrinsic to PV neurons themselves.

In summary, the evoked firing rate of PV neurons is dramatically reduced by brief deprivation in a manner that is developmentally restricted to the critical period. On the other hand, in the adult PV neurons do not initiate cortical rewiring of excitatory network but are likely to reflect more subtle changes in activity patterns generated by the excitatory network after brief deprivation.

ACKNOWLEDGMENTS

We thank Brent Doiron for useful discussions and Ruilin Zhang for technical assistance.

GRANTS

This work was supported by Pennsylvania Department of Health Formula Grant SAP 4100062201 and National Eye Institute Grant R01 EY-024678.

DISCLOSURES

No conflicts of interest, financial or otherwise, are declared by the authors.

AUTHOR CONTRIBUTIONS

B.D.F., M.N.S., and S.J.K. conceived and designed research; B.D.F. and D.E.P. performed experiments; B.D.F., D.E.P., M.N.S., and S.J.K. analyzed data; B.D.F., D.E.P., M.N.S., and S.J.K. interpreted results of experiments; B.D.F., M.N.S., and S.J.K. prepared figures; B.D.F. and S.J.K. drafted manuscript; B.D.F. and S.J.K. edited and revised manuscript; B.D.F. and S.J.K. approved final version of manuscript.

REFERENCES

- Aton SJ, Broussard C, Dumoulin M, Seibt J, Watson A, Coleman T, Frank MG. Visual experience and subsequent sleep induce sequential plastic changes in putative inhibitory and excitatory cortical neurons. *Proc Natl Acad Sci USA* 110: 3101–3106, 2013. doi:10.1073/pnas.1208093110
- Bock DD, Lee WC, Kerlin AM, Andermann ML, Hood G, Wetzel AW, Yurgenson S, Soucy ER, Kim HS, Reid RC. Network anatomy and in vivo physiology of visual cortical neurons. *Nature* 471: 177–182, 2011. doi:10.1038/nature09802.
- Churchland MM, Yu BM, Cunningham JP, Sugrue LP, Cohen MR, Corrado GS, Newsome WT, Clark AM, Hosseini P, Scott BB, Bradley DC, Smith MA, Kohn A, Movshon JA, Armstrong KM, Moore T, Chang SW, Snyder LH, Lisberger SG, Priebe NJ, Finn IM, Ferster D, Ryu SI, Santhanam G, Sahani M, Shenoy KV. Stimulus onset quenches neural variability: a widespread cortical phenomenon. *Nat Neurosci* 13: 369–378, 2010. doi:10.1038/nm.2501.
- Churchland MM, Yu BM, Ryu SI, Santhanam G, Shenoy KV. Neural variability in premotor cortex provides a signature of motor preparation. *J Neurosci* 26: 3697–3712, 2006. doi:10.1523/JNEUROSCI.3762-05.2006.
- Cooper LN, Bear MF. The BCM theory of synapse modification at 30: interaction of theory with experiment. *Nat Rev Neurosci* 13: 798–810, 2012. doi:10.1038/nrn3353.
- D'Souza RD, Burkhalter A. A laminar organization for selective cortico-cortical communication. *Front Neuroanat* 11: 71, 2017. doi:10.3389/fnana.2017.00071.
- Doiron B, Litwin-Kumar A, Rosenbaum R, Ocker GK, Josić K. The mechanics of state-dependent neural correlations. *Nat Neurosci* 19: 383–393, 2016. doi:10.1038/nm.4242.
- Gandhi SP, Yanagawa Y, Stryker MP. Delayed plasticity of inhibitory neurons in developing visual cortex. *Proc Natl Acad Sci USA* 105: 16797–16802, 2008. doi:10.1073/pnas.0806159105.
- Gu Y, Tran T, Murase S, Borrell A, Kirkwood A, Quinlan EM. Neuregulin-dependent regulation of fast-spiking interneuron excitability controls the timing of the critical period. *J Neurosci* 36: 10285–10295, 2016. doi:10.1523/JNEUROSCI.4242-15.2016.
- Han F, Caporale N, Dan Y. Reverberation of recent visual experience in spontaneous cortical waves. *Neuron* 60: 321–327, 2008. doi:10.1016/j.neuron.2008.08.026.
- Hengen KB, Lambo ME, Van Hooser SD, Katz DB, Turrigiano GG. Firing rate homeostasis in visual cortex of freely behaving rodents. *Neuron* 80: 335–342, 2013. doi:10.1016/j.neuron.2013.08.038.
- Hengen KB, Torrado Pacheco A, McGregor JN, Van Hooser SD, Turrigiano GG. Neuronal firing rate homeostasis is inhibited by sleep and promoted by wake. *Cell* 165: 180–191, 2016. doi:10.1016/j.cell.2016.01.046.
- Hensch TK. Critical period plasticity in local cortical circuits. *Nat Rev Neurosci* 6: 877–888, 2005. doi:10.1038/nrn1787.
- Hensch TK, Stryker MP. Columnar architecture sculpted by GABA circuits in developing cat visual cortex. *Science* 303: 1678–1681, 2004. doi:10.1126/science.1091031.
- Jiang B, Huang ZJ, Morales B, Kirkwood A. Maturation of GABAergic transmission and the timing of plasticity in visual cortex. *Brain Res Brain Res Rev* 50: 126–133, 2005. doi:10.1016/j.brainresrev.2005.05.007.
- Kuhlman SJ, Lu J, Lazarus MS, Huang ZJ. Maturation of GABAergic inhibition promotes strengthening of temporally coherent inputs among

- convergent pathways. *PLOS Comput Biol* 6: e1000797, 2010. doi:10.1371/journal.pcbi.1000797.
- Kuhlman SJ, Olivas ND, Tring E, Ikrar T, Xu X, Trachtenberg JT.** A disinhibitory microcircuit initiates critical-period plasticity in the visual cortex. *Nature* 501: 543–546, 2013. doi:10.1038/nature12485.
- Kuhlman SJ, Tring E, Trachtenberg JT.** Fast-spiking interneurons have an initial orientation bias that is lost with vision. *Nat Neurosci* 14: 1121–1123, 2011. doi:10.1038/nn.2890.
- Lambo ME, Turrigiano GG.** Synaptic and intrinsic homeostatic mechanisms cooperate to increase L2/3 pyramidal neuron excitability during a late phase of critical period plasticity. *J Neurosci* 33: 8810–8819, 2013. doi:10.1523/JNEUROSCI.4502-12.2013.
- Litwin-Kumar A, Rosenbaum R, Doiron B.** Inhibitory stabilization and visual coding in cortical circuits with multiple interneuron subtypes. *J Neurophysiol* 115: 1399–1409, 2016. doi:10.1152/jn.00732.2015.
- Liu BH, Li P, Li YT, Sun YJ, Yanagawa Y, Obata K, Zhang LI, Tao HW.** Visual receptive field structure of cortical inhibitory neurons revealed by two-photon imaging guided recording. *J Neurosci* 29: 10520–10532, 2009. doi:10.1523/JNEUROSCI.1915-09.2009.
- Luczak A, Barthó P, Harris KD.** Spontaneous events outline the realm of possible sensory responses in neocortical populations. *Neuron* 62: 413–425, 2009. doi:10.1016/j.neuron.2009.03.014.
- Ma WP, Liu BH, Li YT, Huang ZJ, Zhang LI, Tao HW.** Visual representations by cortical somatostatin inhibitory neurons—selective but with weak and delayed responses. *J Neurosci* 30: 14371–14379, 2010. doi:10.1523/JNEUROSCI.3248-10.2010.
- Mitchell JF, Sundberg KA, Reynolds JH.** Differential attention-dependent response modulation across cell classes in macaque visual area V4. *Neuron* 55: 131–141, 2007. doi:10.1016/j.neuron.2007.06.018.
- Monier C, Chavane F, Baudot P, Graham LJ, Frégnac Y.** Orientation and direction selectivity of synaptic inputs in visual cortical neurons: a diversity of combinations produces spike tuning. *Neuron* 37: 663–680, 2003. doi:10.1016/S0896-6273(03)00064-3.
- Nataraj K, Turrigiano G.** Regional and temporal specificity of intrinsic plasticity mechanisms in rodent primary visual cortex. *J Neurosci* 31: 17932–17940, 2011. doi:10.1523/JNEUROSCI.4455-11.2011.
- Nawrot MP, Boucsein C, Rodriguez Molina V, Riehle A, Aertsen A, Rotter S.** Measurement of variability dynamics in cortical spike trains. *J Neurosci Methods* 169: 374–390, 2008. doi:10.1016/j.jneumeth.2007.10.013.
- Pologruto TA, Sabatini BL, Svoboda K.** ScanImage: flexible software for operating laser scanning microscopes. *Biomed Eng Online* 2: 13, 2003. doi:10.1186/1475-925X-2-13.
- Pouille F, Marin-Burgin A, Adesnik H, Atallah BV, Scanziani M.** Input normalization by global feedforward inhibition expands cortical dynamic range. *Nat Neurosci* 12: 1577–1585, 2009. doi:10.1038/nn.2441.
- Poulet JF, Petersen CC.** Internal brain state regulates membrane potential synchrony in barrel cortex of behaving mice. *Nature* 454: 881–885, 2008. doi:10.1038/nature07150.
- Ringach DL.** Spontaneous and driven cortical activity: implications for computation. *Curr Opin Neurobiol* 19: 439–444, 2009. doi:10.1016/j.conb.2009.07.005.
- Ringach DL, Shapley RM, Hawken MJ.** Orientation selectivity in macaque V1: diversity and laminar dependence. *J Neurosci* 22: 5639–5651, 2002.
- Shadlen MN, Newsome WT.** The variable discharge of cortical neurons: implications for connectivity, computation, and information coding. *J Neurosci* 18: 3870–3896, 1998.
- Stephany CE, Ikrar T, Nguyen C, Xu X, McGee AW.** nogo receptor 1 confines a disinhibitory microcircuit to the critical period in visual cortex. *J Neurosci* 36: 11006–11012, 2016. doi:10.1523/JNEUROSCI.0935-16.2016.
- Sun Y, Ikrar T, Davis MF, Gong N, Zheng X, Luo ZD, Lai C, Mei L, Holmes TC, Gandhi SP, Xu X.** Neuregulin-1/ErbB4 signaling regulates visual cortical plasticity. *Neuron* 92: 160–173, 2016. doi:10.1016/j.neuron.2016.08.033.
- Sussillo D, Abbott LF.** Generating coherent patterns of activity from chaotic neural networks. *Neuron* 63: 544–557, 2009. doi:10.1016/j.neuron.2009.07.018.
- van Versendaal D, Levelt CN.** Inhibitory interneurons in visual cortical plasticity. *Cell Mol Life Sci* 73: 3677–3691, 2016. doi:10.1007/s00018-016-2264-4.
- Wang Q, Burkhalter A.** Area map of mouse visual cortex. *J Comp Neurol* 502: 339–357, 2007. doi:10.1002/cne.21286.
- Yazaki-Sugiyama Y, Kang S, Câteau H, Fukai T, Hensch TK.** Bidirectional plasticity in fast-spiking GABA circuits by visual experience. *Nature* 462: 218–221, 2009. doi:10.1038/nature08485.